JOURNAL OF SPACECRAFT AND ROCKETS
Vol. 34, No. 1, January–February 1997

New Semiempirical Model for Wing–Tail Interference

F. G. Moore* and R. M. McInville†
U.S. Naval Surface Warfare Center, Dahlgren, Virginia 22448-5000

A new semiempirical model to predict wing–tail interference on missile configurations has been developed. The new model is grounded in slender body theory at low angle of attack and uses experimental data at high angle of attack to estimate the interference term as a percent of slender body theory. The theory is developed for the roll position of both 0 deg [fins in plus (+) fin arrangement] and 45 deg [fins in cross (×) fin arrangement]. Comparison of the new method to existing approaches and experimental data appears to show the new technique to be a potential improvement in the state of the art for wing–tail interference prediction methods. However, additional wind-tunnel data for wing–tail interference are needed for evaluation of the new model before definitive statements can be made on its added value and, in particular, its accuracy outside the range of data upon which it was based.

Nomenclature

AR	= aspect ratio, b^2/A_W
A_{REF}	= reference area (maximum cross-sectional area of body, if a body is present, or planform area of wing, if wing alone), ft^2
b	= wing span (not including body), ft
C_M	= pitching moment coefficient (based on reference area and body diameter)
$C_{N_{T(V)}}$	= negative normal-force coefficient component on tail due to wing- or canard-shed vortex
C_{N_W}, C_{N_T}	= normal-force coefficient of wing or tail alone
C_{N_α}	= normal-force coefficient derivative
E_1, E_2, G_1	= constants used in semiempirical wing–tail interference model
f_W, f_T	= lateral location of wing or tail vortex (measured in feet from body centerline)
i	= tail interference factor
$K_{W(B)}$, $K_{T(B)}$	= ratio of normal-force coefficient of wing or tail in presence of body to that of wing or tail alone at $\delta = 0$ deg
M	= Mach number, V/a
P_l, P_W	= loading factors in leeward and windward planes, respectively
r_W, r_T	= radius of body at wing or tail locations
s	= wing or tail semispan plus the body radius in wing–body lift methodology
α	= angle of attack, deg
α_F	= value of α (as percent of α_N) where $C_{N_{T(V)}}$ reaches a maximum magnitude
α_N	= value of α where $C_{N_{T(V)}}$ goes to zero
α_{N_0}	= value of α where $C_{N_{T(V)}}$ goes to zero for $A_W/A_{\text{REF}} = 5.5$
Φ	= circumferential location around body where $\Phi = 0$ is leeward plane with fins in plus fin arrangement, deg

Introduction

THE 1995 version of the U.S. Naval Surface Warfare Center, Dahlgren Division, aeroprediction code[1] (AP95) has recently been extended to the roll position of $\Phi = 45$ deg (fins in cross or × fin arrangement).[2] During the course of this investigation, the author found some actual wind-tunnel data[3–5] that measured the wing–tail interference term when there were no control deflections. Also included in Ref. 3 were comparisons of several available theoretical methods for predicting wing–tail interference. In examining the comparisons of these methods to the data, along with the recently developed AP95,[1] it was concluded that additional improvements in wing–tail interference methods were needed. As a result of this conclusion, an attempt was made to develop a new semiempirical method for wing–tail interference that is applicable to the range of variables over which the AP95 operates. These variables include Mach numbers up to 20, angles of attack (AOA) up to 90 deg, and $\Phi = 0$ deg roll. Because we were in the process of extending the AP95 to the $\Phi = 45$ deg roll position, it was also decided to attempt to develop the semiempirical method for that roll position as well.

The present paper will briefly describe elements of slender body theory (SBT), upon which the method is developed, and then define the semiempirical parameters needed to extend the SBT to higher AOA and Mach number. It will then compare the new theory with existing theories and the AP95 on a limited number of configurations to confirm the improvements afforded by the new method. This paper will deal with the case where control deflections are zero. A companion paper, also based on Ref. 2, will define the nonlinear interference factors due to AOA and control deflection for both the $\Phi = 0$ and 45 deg roll positions.

Analysis

Summary of SBT

The wing–tail interference normal force as defined by line vortex and SBT[2,6] for no forward control surface deflection is

$$C_{N_{T(V)}} = \frac{A_W \left(C_{N_\alpha}\right)_W \left(C_{N_\alpha}\right)_T K_{W(B)} \alpha (s_T - r_T)}{2\pi (AR)_T (f_W - r_W) A_{\text{REF}}} \times (i_1 \cos\Phi + i_4 \sin\Phi) \tag{1}$$

Equation (1) is derived assuming one vortex per forward wing panel streams back along the velocity vector toward the tail panels. The point where the vortices are shed from the wings, f_W, is calculated by SBT and is approximately $\pi/4$ times the semispan of the wing. The interference factors i_1 and i_4 are nondimensional measures of the interference of a vortex on a lifting surface. Generally, strip theory (or two-dimensional flow over sections of the tail) is used to calculate the values of i. The values of i are functions of the geometry of the wing and tail because the velocity, vortex strengths, etc., have all been nondimensionalized out of the equation for i. On the other hand, Eq. (1) is a function of Mach number due to the fact that linear theory is normally used to compute the normal force coefficient derivatives of the wing and tail.

If the configuration is at $\Phi = 0$ deg roll, only two wings will shed vortices. To satisfy the boundary condition on the body surface of zero normal velocity, an image vortex of equal and opposite strength to those on the wings must be placed on the radius vector along

Received Feb. 7, 1996; revision received July 1, 1996; presented as Paper 96-3393 at the AIAA Atmospheric Flight Mechanics Conference, San Diego, CA, July 29–31, 1996; accepted for publication Oct. 5, 1996.

*Senior Aerodynamicist, Weapons Systems Department, Dahlgren Division. Associate Fellow AIAA.

†Aerospace Engineer, Aeromechanics Branch, Weapons Systems Department, Dahlgren Division.

the body centroid to the wing vortex. As a result, four or eight total vortices must be accounted for in the $\Phi = 0$ or 45 deg roll positions, respectively. For simplicity, these vortices are assumed to stream back to the tail fins following the velocity vector. The interference factors i_1 and i_4 of Eq. (1) are strongly dependent on the height of the vortices above the tail fins. A complicated expression for this height is given in Ref. 2.

Referring back to Eq. (1), i_1 represents the interference factor emanating from the windward plane fin and i_4 the interference factor of the leeward plane fin. Since the configuration is symmetric, only fins 1 and 4 need to be considered and a factor of 2 included in the equations for i (Ref. 2). If the vehicle is in the $\Phi = 0$ deg roll position, then only i_1 of Eq. (1) is included and Eq. (1) reduces to the more conventional methodology as given in Ref. 7. In the computation of the interference factors, it is generally assumed that the vortex strength from fin 1 is the negative of that of fin 3 (Ref. 6) and similar for fins 2 and 4.

In utilizing the SBT for several wing–tail configurations, the following conclusions were reached in comparison to experiment.[2]

1) SBT generally gives a reasonable estimate of $C_{N_{T(V)}}$ for low AOA for both the $\Phi = 0$ and 45 deg roll positions. It tends to give slightly low values of $C_{N_{T(V)}}$ for Mach numbers less than about 2.0 and slightly high for Mach numbers greater than 2.0.

2) For AOAs greater than about 10 deg, SBT tends to give values of $C_{N_{T(V)}}$ that are generally higher than experiment. The higher the Mach number or AOA, the worse the predictions.

Although these conclusions are encouraging at low AOA, the accuracy at higher AOA and Mach number is not too surprising given the assumptions inherent in SBT. SBT basically assumes crosswise dimensions of span or thickness are small compared with length. Mathematically, this assumption leads to the result of Mach number independence for bodies and wings alone or in combination as well as a linear dependence on AOA. Hence, SBT cannot be relied upon to predict the nonlinearities associated with nonslender bodies (which most weapons are at some local points), higher AOA, or strong compressibility effects.

Reference 3 also showed comparisons of wing–tail interference with several other methods. Although some of the methods showed improvement over SBT, none were as accurate as desired. As a result, new semiempirical methods were developed, based on SBT at low AOA and data plus SBT at higher AOA, to predict $C_{N_{T(V)}}$ at both the $\Phi = 0$ and 45 deg roll positions.

In an effort to improve upon the existing state-of-the-art wing–tail methodology, the literature was searched for wing–tail interference data. References 3 and 4 were found in this process. These references documented wind-tunnel tests on two different missile configurations in which actual wing–tail normal-force measurements were made. Reference 3 measured these results on individual fins as a function of roll position at Mach numbers of 2, 3, and 4. Reference 4 gave results for only the $\Phi = 0$ deg roll position at $M_\infty = 1.1$. Figure 1a shows the configuration tested in Ref. 3 along with results at $M_\infty = 1.95$ and 4.02 at roll position of 0 deg. Also reported in Ref. 3 were the theoretical computations from analytical codes referred to as AERODSN,[3] MISSILE 2A,[6] and LRCDM.[7] According to Ref. 3, the AERODSN code has the same wing–tail interference model as the older version of the aeroprediction code and is based on SBT from Ref. 8. The MISSILE 2A program is based on theory and experiment and, therefore, should contain some of the nonlinearity associated with the wing–tail interference. The LRCDM code is based on paneling methods and databases and therefore should also contain some of the nonlinearities of the wing–tail interference. For comparison purposes, $C_{N_{T(V)}}$ computed by the AP95 for a single fin is also shown in Figs. 1b and 1c. The AP95, although it contains some nonlinearities, still resembles the SBT, as seen from the close proximity to the AERODSN results. It is fair to say, in viewing the comparison of the various theoretical approaches for predicting wing–tail interference in Fig. 1, that improvements in the theory are needed.

A model for no control deflection, based on a third-order equation in AOA, is postulated to fit the data from both Refs. 3 and 4. This model is defined by

$$\left[C_{N_{T(V)}}\right]_\alpha = A + B\alpha + C\alpha^2 + D\alpha^3 \tag{2}$$

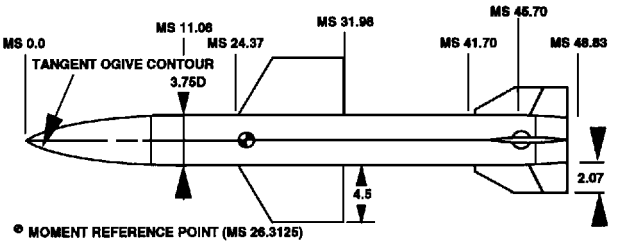

a) Configuration tested in Ref. 3

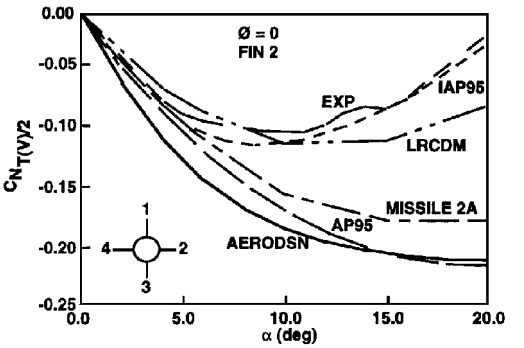

b) Single fin wing–tail interference ($M = 1.96$)

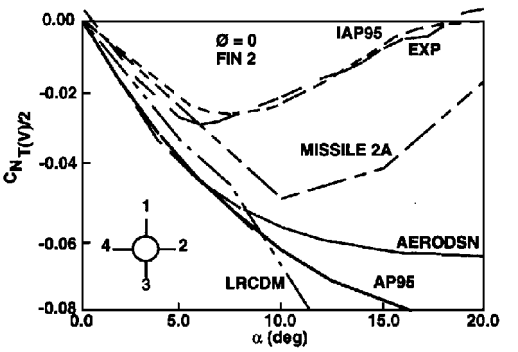

c) Single fin wing–tail interference ($M = 4.02$)

Fig. 1 Configuration and single fin data from Ref. 3 for wing–tail interference normal force. All dimensions in inches unless otherwise stated.

The four constants of Eq. (2) require four conditions to define them. These conditions are as follows.

1) The wings are assumed to be thin and disturb the flow slightly so that $C_{N_{T(V)}} = 0$ at $\alpha = 0$.

2) The slope of SBT value for $C_{N_{T(V)}}$ near $\alpha = 0$ is required (using this value and a value of the real slope from data, a modified value of this slope can be obtained).

3) The AOA where $C_{N_{T(V)}}$ goes to zero based on data is needed.

4) Finally, the maximum value of $C_{N_{T(V)}}$ as a percent of SBT at AOA where $C_{N_{T(V)}}$ is a maximum is required.

Note in the four conditions chosen, SBT is used twice. Based on these conditions, the four constants of Eq. (2) become

$$A = 0 \tag{3}$$

$$B = \left[\left(\frac{\mathrm{d}C_{N_{T(V)}}}{\mathrm{d}\alpha}\right)_{\alpha=0}\right]_{\mathrm{SBT}} E_1 \tag{4}$$

$$C = \frac{-B - D\alpha_N^2}{\alpha_N} \tag{5}$$

$$D = \frac{E_2\alpha_N - B\alpha_N\alpha_F + B\alpha_F^2}{\alpha_N\alpha_F^3 - \alpha_F^2\alpha_N^2} \tag{6}$$

The parameters in the constants B, C, and D are defined as follows, based on Fig. 2:

α_{N_0} = value from Fig. 2a

α_F = (value from Fig. 2b)$\times(\alpha_N/100)$

E_1 = value from Fig. 2c

E_2 = (value from Fig. 2d) $\times$ $([C_{N_{T(V)}}]_{\mathrm{SBT}})_{\alpha=\alpha_F}$

The question arises regarding how to account for fins that are of sizes and locations different from those tested in Refs. 3 and 4. Fortunately, both fins tested in these references were significantly larger than the tail surfaces and were located in a wing vs a canard location. Hence, the present approach will be to use these results directly for wings or canards of less area-to-body reference area than those tested. For wings of greater area, it is assumed that the AOA, α_N, where the $C_{N_{T(V)}}$ becomes negligible is increased according to

$$\alpha_N = \alpha_{N_0} \quad \text{for} \quad \frac{A_W}{A_{\mathrm{REF}}} \le 5.5$$
$$\alpha_N = \alpha_{N_0}\left(\frac{A_W/A_{\mathrm{REF}}}{5.5}\right) \quad \text{for} \quad \frac{A_W}{A_{\mathrm{REF}}} > 5.5 \tag{7}$$

with an upper limit on α_N of 2.5 α_{N_0}.

The value of A_W/A_{REF} of 5.5 corresponds to the wing area ratio of Ref. 3. Also, for wings larger than those of Ref. 3, an upper limit on the amount of lift loss on the tail will remain in effect. This upper limit is defined by the following methodology.

For $M \le 1.5$:

$$\frac{|C_{N_{T(V)}}|}{C_{N_T}} = 1.0; \qquad \alpha \le 5$$
$$\frac{|C_{N_{T(V)}}|}{C_{N_T}} = 1.0 - 0.04125(\alpha - 5); \qquad \alpha > 5 \tag{8a}$$

For $1.5 < M \le 2.5$:

$$\frac{|C_{N_{T(V)}}|}{C_{N_T}} = 0.9 - 0.025\alpha; \qquad \alpha \le 10$$
$$\frac{|C_{N_{T(V)}}|}{C_{N_T}} = 0.65 - 0.0235(\alpha - 10); \qquad \alpha > 10 \tag{8b}$$

For $M > 2.5$:

$$\frac{|C_{N_{T(V)}}|}{C_{N_T}} = 0.8 - 0.025\alpha \tag{8c}$$

where α is AOA in degrees. Equation (8a) says that at $\alpha = 0$ deg the maximum lift loss on the tail is limited to 100% of the tail lift, regardless of the size of the wings. The percent lift loss then decreases linearly with AOA as defined by Eqs. (8a–8c).

Admittedly, this methodology is conservative (overpredicts $C_{N_{T(V)}}$) for values of $A_W/A_{\mathrm{REF}} < 5.5$ and is simply a judgment based on numerical experiments for values of $A_W/A_{\mathrm{REF}} > 5.5$. However, this overprediction is less than it would be using the AP95 methodology for wing–tail interference methodology. It does accomplish the objective of making the wing-tail interference with no control deflection more closely approximate data than available approaches, including the AP95. This fact is illustrated by the results shown in Figs. 1b and 1c for the improved aeropredictioncode 1995 (IAP95).

Before moving to the wing–tail interference methodology for the $\Phi = 45$ deg roll position, a comment would be valuable on the Fig. 2 results, which basically compare SBT with data. First of all, it is clear that at low AOA SBT underpredicts $C_{N_{T(V)}}$ for low Mach numbers and overpredicts it at high Mach numbers, for the Ref. 3 configuration. The point of optimum prediction appears to be around Mach 2 (see Fig. 2c). Second, the $C_{N_{T(V)}}$ term decays much faster at high AOA than does SBT. This is increasingly true as Mach number increases. This again highlights the Newtonian impact assumptions at high Mach number where in the leeward plane

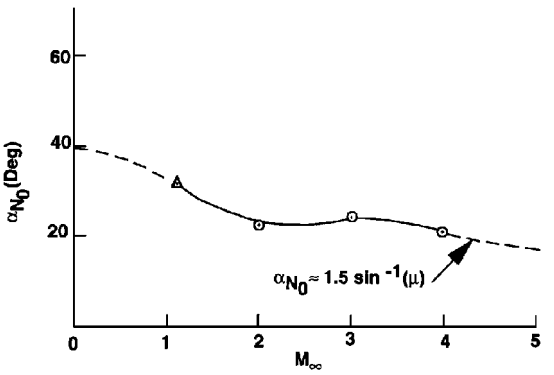

Fig. 2a AOA where wing–tail interference is negligible.

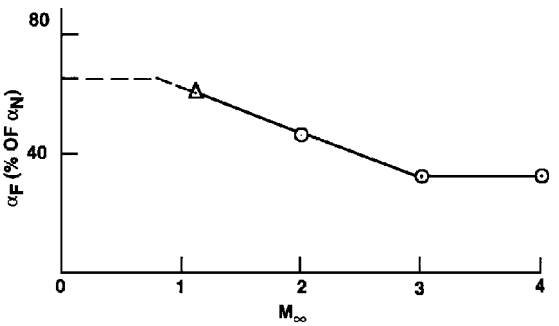

Fig. 2b AOA where wing–tail interference is a maximum (percent of α_N).

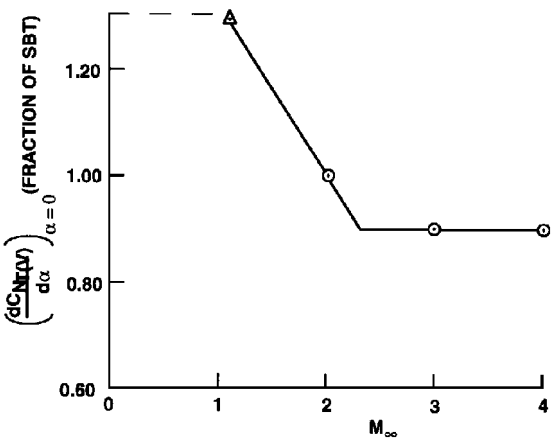

Fig. 2c Initial slope at $\alpha = 0$ deg of wing–tail interference as a function of M_∞.

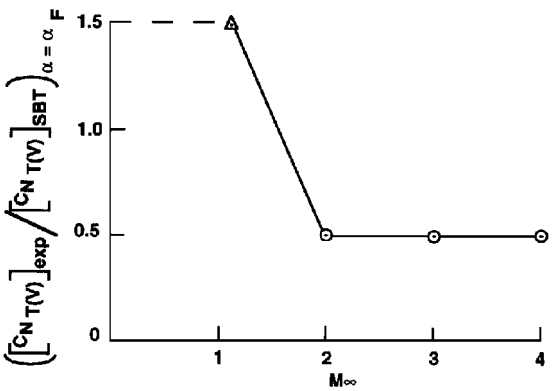

Fig. 2d Slender body theory prediction of wing–tail interference at AOA where $[C_{N_{T(V)}}]_{\mathrm{exp}}$ reaches a maximum.

vortex effects are completely dominated by the dynamic pressure in the windward plane. Figures 1b, 1c, and 2a illustrate this fact, showing that the AOA where $C_{N_{T(V)}}$ is negligible gets smaller as M_∞ increases; also, the maximum magnitude as a percent of SBT gets smaller with increasing M_∞. The SBT representation of the wing–tail interference for $\Phi = 45$ deg roll makes the assumption that the strength of the vortex shed from the windward plane fins is equal in magnitude and opposite in direction to the leeward plane fins. At small AOA, this assumption is quite reasonable and is partially what leads to the fact that cruciform wing–body–tail missile aerodynamics are independent of roll position. As AOA increases, this assumption becomes less and less valid. In fact, the lift of the windward plane fin is much larger than the leeward plane fin as AOA increases. This differential in normal force was modeled approximately in the center of pressure shift discussed in Ref. 2 by approximating a linear variation in the shift of normal force to the windward plane fin from the leeward plane fin up to AOA 65 deg. At that point, the ratio of the windward to leeward plane load remained constant.

If we define the factors

$$P_W = [1.0 + 0.8(\alpha/65)], \quad P_l = [1.0 - 0.8(\alpha/65)]$$

$$\alpha \le 65, \qquad P_W = 1.8, \qquad P_l = 0.2; \qquad \alpha > 65 \quad (9)$$

then the interference factors can be weighted by Eq. (9) depending on where the vortex is shed. If it is shed in the windward plane, then the P_W factor is appropriate, whereas if it is shed from the leeward plane, then the P_ℓ factor in Eq. (9) is appropriate. This is an approximate way to represent the nonlinear nature of the load in the windward to leeward plane fin and the strength of the vorticity shed from each fin.

The slender body equations for computing the interference factors i_1 and i_4 for the fins in the windward and leeward planes are quite lengthy and will not be repeated here. The interested reader is referred to Ref. 2 for these equations. However, the main new ingredient in this paper in computing the interference factors is the weighting of the windward and leeward plane vortices by the factors given by Eq. (9). Knowing the weighted values of i_1 and i_4, the modified values of wing–tail interference using SBT can be computed by Eq. (1) for $\Phi = 45$ deg roll.

The final two modifications for inclusion of nonlinearities into the wing–tail interference model for the $\Phi = 45$ deg roll position are to adjust Eq. (1) based on experimental data analogous to the $\Phi = 0$ deg methodology of Fig. 2. For the 45 deg roll position, the only data found on individual fins were from Ref. 3. Figure 3 gives the $C_{N_{T(V)}}$ values for M_∞ values of 1.95, 3.01, and 4.02. In developing an analogous model to Fig. 2 for $\Phi = 45$ deg, qualitative use will be made of the $\Phi = 0$ deg results at lower Mach number because at least one set of data existed for $M_\infty = 1.1$. These results will be used to compare trends of data as a function of Mach number and AOA, not their absolute values.

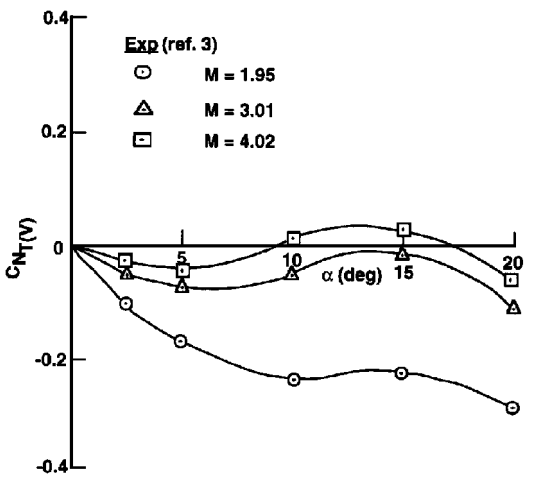

Fig. 3 Wing–tail interference ($\Phi = 45$ deg, $\delta = 0$ deg).

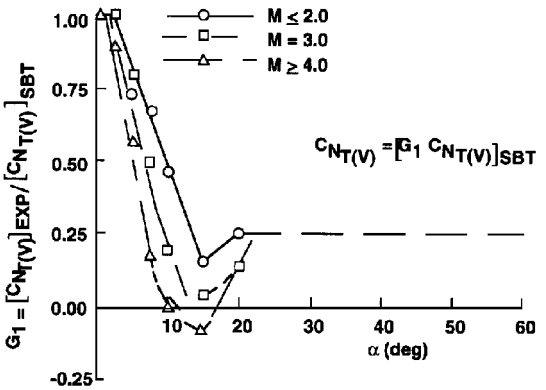

Fig. 4 Wing–tail interference model for no control deflection at $\Phi = 45$ deg.

The curves of Fig. 3 show a point of inflection in the experimental data between 10 and 15-deg AOA. This is because at very low AOA the windward and leeward plane vortices shed from the wings adversely impact the tail normal force. However, at a slightly higher AOA, the windward plane wing-shed vortex has a positive effect on the leeward plane tail because of the counterclockwise vortex hitting the windward side of the leeward tail surface. As the AOA is increased higher, the wing-shed windward plane vortex rises above the leeward plane tail fin. At this point, both wing-shed vortices again have an adverse impact on the tail normal force. This is because both wing shed vortices are above both tail fins and have downward velocities on both fins, thus decreasing the tail normal force on each fin.

Although a model such as that derived for the $\Phi = 0$ deg roll position could be derived for the $\Phi = 45$ deg plane, it is more difficult because of a lack of data below $M_\infty = 2.0$ and the shape of the curves in Fig. 3. As a result, modified SBT was used to calculate $C_{N_{T(V)}}$ at various AOAs and at the three Mach numbers where data were available. The results were compared with the experimental data of Fig. 3, and the semiempirical model of Fig. 4 was defined for no control deflection.

Referring to Eq. (1), the model for $\Phi = 45$ deg roll for no control deflection is then

$$C_{N_{T(V)}} = G_1\left[C_{N_{T(V)}}\right]_{\text{SBT}} \quad (10)$$

where $[C_{N_{T(V)}}]_{\text{SBT}}$ is the value from Eq. (1) where the loading factors of Eq. (9) have been included and G_1 is the value from Fig. 4.

Note that the curves for $M = 2$ and 4 data are used in the AP95 code for $M \le 2$ and ≥ 4, respectively. This use does not imply the data taken are for those Mach numbers. Rather it implies a use of the data at $M = 2$ and 4 for Mach numbers outside this range to allow the AP95 to compute wing–tail interference at all Mach numbers. We hope additional data will become available and a refined model can be created at that time.

The other modification to the SBT for the $\Phi = 45$ deg roll position is to include the same fin size and maximum value constraints given by Eqs. (7) and (8). With all of these modifications, the new semiempirical model for the $\Phi = 45$ deg roll will closely duplicate the experimental results in Fig. 3.

Results and Discussion

The only explicit wing–tail data the authors found were given in Refs. 3 and 4. Some of these data are given in Figs. 1 and 3. As seen in Fig. 1, the semiempirical model labeled IAP95 basically duplicates the wind-tunnel data for $\Phi = 0$ deg. Although the IAP95 is not shown in Fig. 3 for clarity, the same is basically true for that case where $\Phi = 45$ deg as well. Since additional data for $C_{N_{T(V)}}$ were not available, the next best validation of the new semiempirical model is to investigate the potential improvements of the new model on total missile aerodynamics. The aerodynamic term of most interest is the pitching moment, because the $C_{N_{T(V)}}$ is fairly small. Hence, normal force is little affected, but pitching moment, due to generally long moment arms, is more strongly impacted.

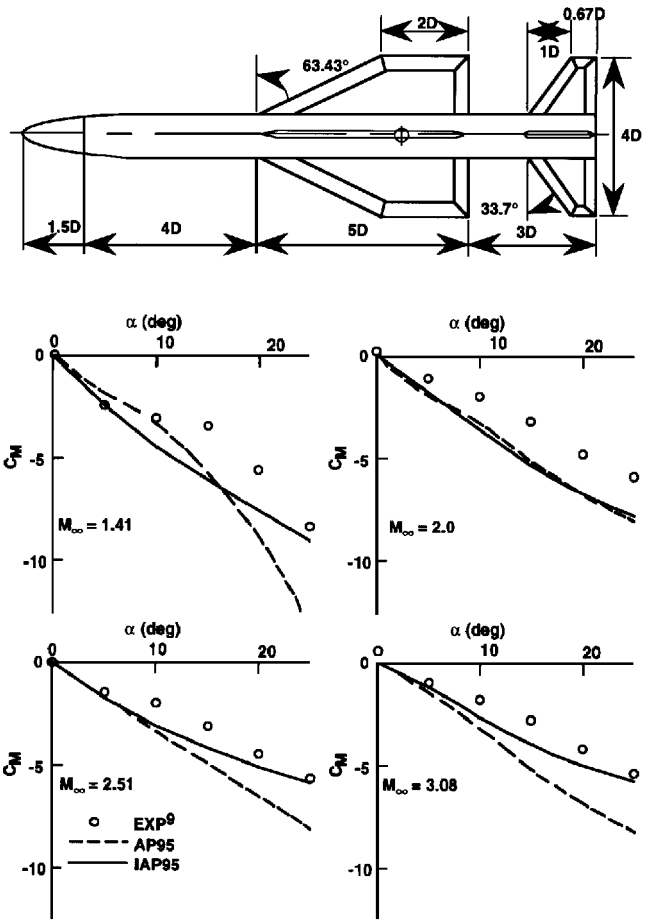

Fig. 5 Comparison of theory and experiment for pitching moment coefficient (Φ = 0 deg).

Two cases are chosen for this validation, both of which have fairly large wings in relatively close proximity to the tail. The first case is shown in Fig. 5 and is taken from Ref. 9. Data from Ref. 9 were only available for $\Phi = 0$ at 0–25 deg AOA over the Mach range 1.4–3.08. However, this should be a reasonable test for the new methodology. As seen in Fig. 5, the new wing–tail model gives some improvement in pitching moment coefficient predictions over the AP95 model. The improvements are naturally the most noticeable at higher AOA and Mach number where the AP95, which still resembles SBT, is most inaccurate. There is basically no improvement in the IAP95 over the AP95 at $M = 2.0$.

As already mentioned and shown in Fig. 2c, SBT appears to be near optimum at low AOA and around $M = 2$. Thus the new semiempirical model deviates very little from the AP95 at this Mach number.

The last case is for the Seasparrow missile configuration as tested in Ref. 10 and shown in Fig. 6. Figure 6 gives pitching moment coefficients for no control deflection at $M_\infty = 1.5$, 2.87, and 4.63 for AOAs to 40 deg. Both the $\Phi = 0$ and 45 deg results are shown. However, only the IAP95 predictions are given because the AP95 is not applicable to the $\Phi = 45$ deg roll orientation. In general, very acceptable agreement is obtained between the theory and experiment at all conditions except at $M = 4.63$ above an AOA of 35 deg. Around AOA of 30 deg, it is believed the bow shock intersects the wings, creating a trailing shock that intersects the tail surfaces. These internal shock interactions cause a sudden loss of tail normal force and resultant stability. This physical phenomenon is not modeled in the IAP95. Although not shown, the IAP95 gives as good or better results than the AP95 at $\Phi = 0$ deg. Also, the IAP95 predicts the $\Phi = 45$ deg pitching moment slightly better than the $\Phi = 0$ deg results. This is primarily due to a center of pressure shift for wing lift at $\Phi = 45$ deg discussed in Ref. 2.

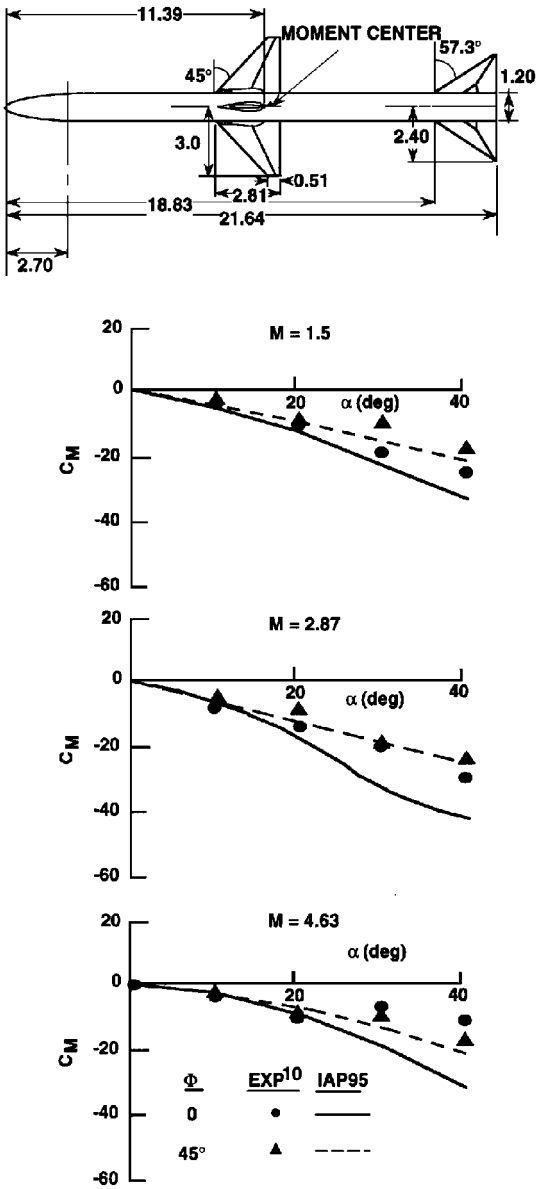

Fig. 6 Seasparrow pitching moment coefficient comparison of experiment and IAP95.

Summary

A new semiempirical wing–tail interference model has been developed based on slender body theory and experimental data. The method was developed so that it could be applied to the Mach number (0–20) and AOA (0–90 deg) range for which the AP95 code was designed. Only limited wing–tail interference data were found in the literature. It is believed the current semiempirical method could be refined and improved with additional data. This is particularly true at AOA and Mach numbers outside the range of data on which the method was based.

Comparisons of the new method with total forces and moments on a limited number of wing–body–tail configurations showed the new method to be superior to the AP95 and to other approaches available in the literature. Further verification is needed on other cases before this conclusion can be made in a more definitive sense.

Acknowledgments

The work described in this report was supported through the U.S. Office of Naval Research (Dave Siegel) by the following programs: the Air Launched Weapons Program managed at the Naval Air Warfare Center, China Lake, California, by Tom Loftus and Craig Porter, and the Surface Weapons Systems Technology Program managed at the U.S. Naval Surface Warfare Center, Dahlgren Division (NSWCDD), by Robin Staton and Gil Graff. Also, some support was provided in fiscal year 1994 by the Army Missile Command

at Huntsville, Alabama, under Dave Washington, and in fiscal year 1995 by the Marine Corps Weaponry Technology Program managed at NSWCDD by Bob Stiegler. The authors express appreciation for support received in this work. Appreciation is also given to Tom Hymer, who provided some data used in the validation process.

References

[1]Moore, F. G., McInville, R. M., and Hymer, J. C., "The 1995 Version of the NSWC Aeroprediction Code: Part I—Summary of New Theoretical Methodology," U.S. Naval Surface Warfare Center, NSWCDD/TR-94/379, Dahlgren, VA, Feb. 1995.

[2]Moore, F., and McInville, R., "Extension of the NSWCDD Aeroprediction Code to the Roll Position of 45 Degrees," U.S. Naval Surface Warfare Center, NSWCDD/TR-96/160, Dahlgren, VA, Dec. 1995.

[3]Washington, W. D., and Spring, D. J., "An Experimental Investigation of Wing–Tail Interference for a Typical Supersonic Missile," AIAA Paper 82-1339, Aug. 1982.

[4]Aiello, G. F., and Bateman, M. C., "Aerodynamic Stability Technology for Maneuverable Missiles, Vol. I, Configuration Aerodynamic Characteristics," U.S. Air Force Flight Dynamics Lab., AFFDL-TR-76-55, Vol. 1, Wright–Patterson AFB, OH, March 1979.

[5]Washington, W. D., "Computer Program for Estimating Stability Derivatives of Missile Configurations," U.S. Army Missile Command, TR RD-76-25, Redstone Arsenal, AL, May 1976.

[6]Hemsch, M. J., and Mullen, J., Jr., "Analytical Extension of the MISSILE1 and MISSILE2 Computer Programs," Nielsen Engineering and Research, Inc., TR-272, Mountain View, CA, March 1982.

[7]Dillenius, M. F. E., Hemsch, M. J., Sawyer, W. C., Allen, J. M., and Blair, A. B., Jr., "Comprehensive Missile Aerodynamics Programs for Preliminary Design," AIAA Paper 82-0375, Jan. 1982.

[8]Pitts, W. C., Nielsen, J. N., and Kaaturi, G. E., "Lift and Center of Pressure of Wing-Body-Tail Combinations at Subsonic, Transonic, and Supersonic Speeds," NACA TR 1307, 1957.

[9]Gudmundson, S. E., and Torngren, L., "Supersonic and Transonic Wind Tunnel Tests of Slender Ogive-Cylinder Body Single and in Combination with Cruciform Wings and Tails of Different Sizes," Aeronautical Research Inst. of Sweden, TN FFA AU-772, Stockholm, Sweden, 1972.

[10]Monta, W. J., "Supersonic Aerodynamic Characteristics of a Sparrow III Type Missile Model with Wing Controls and Comparison with Existing Tail Control Results," NASA TP 1078, Nov. 1977.

R. M. Cummings
Associate Editor